Electronic Supplementary Material (ESI) for Journal of Materials Chemistry C.

Electronic Supporting Information

Pyridinium salt with crystalline phase transformation under water vapor and reversible mechanochromism luminescent property

Y. Chen, X. Li, Dr. W. Che, L. Tu, Dr. Y. Xie, Prof. Z. Li

Institute of Molecular Aggregation Science, Tianjin University, Tianjin 300072, China
E-mail: xieyujun@tju.edu.cn;
lizhentju@tju.edu.cn or lizhen@whu.edu.cn.
Prof. Z. Li
Joint School of National University of Singapore and Tianjin University, International Campus of Tianjin University, Binhai New City, Fuzhou 350207, China
Department of Chemistry, Wuhan University, Wuhan 430072, China

Experimental section

Reagents and materials

All reagents and solvents were purchased from commercial sources, *N,N*-dimethylformamide (DMF) was further dried over by refluxing with Calcium hydride then collected under vacuum distillation before use.

Computational study

(TD)DFT calculation is performed on Gaussian 09 program (Revision D.01).[1] The ground state (S_0) geometry is optimized with the Becke's three-parameter exchange functional along with the Lee Yang Parr's correlation functional (B3LYP) using 6-31G(d) basis sets. While geometry at excited state (S_1) is optimized via TDDFT based on S_0 geometry. The excitation energies in the *n*-th singlet (S_n) states is revised by function of CAM-B3LYP.

Measurements

Nuclear magnetic resonance (^{1}H and ^{13}C NMR) spectra were obtained on a Bruker Ultra Shield plus 400 MHz spectrometer. Differential Scanning Calorimetry (DSC) curves were obtained with a NETZSCH DSC 214 thermal analyzer at the heating and cooling rate of 10 K min^{-1} under N_2 atmosphere. Thermogravimetric analyses (TGA) were recorded with a NETZSCH TG 209F3 thermal analyzer under nitrogen atmosphere with a heating rate of 10 K min^{-1}. The powder X-ray diffraction patterns were recorded by RIGAKU SMARTLAB9KW with an X-ray source of Cu Kα (λ = 1.5418 Å) at 298 K at 50 KV and 15 mA at a scan rate of 10^o (2θ) min^{-1} (scan range: 3-60°). X-ray Single crystal diffraction for compounds data was performed on a diffractometer with CCD detector using Cu Kα radiation (λ= 1.5418 Å) source. UV-vis spectra were performed on a Shimadzu UV-2600. The steady-state fluorescence and phosphorescence spectra measurement were carried out by Hitachi F-4700 at 298 K and 77 K respectively. Commission internationale de l'éclairage (CIE) chromaticity coordinates images are calculated and drawn by CIE1931xy software based on the PL spectra. The lifetime and time-resolved emission spectra and PL quantum yield (PLQY) were obtained on Edinburgh FLS1000 fluorescence spectrophotometer.

Synthesis

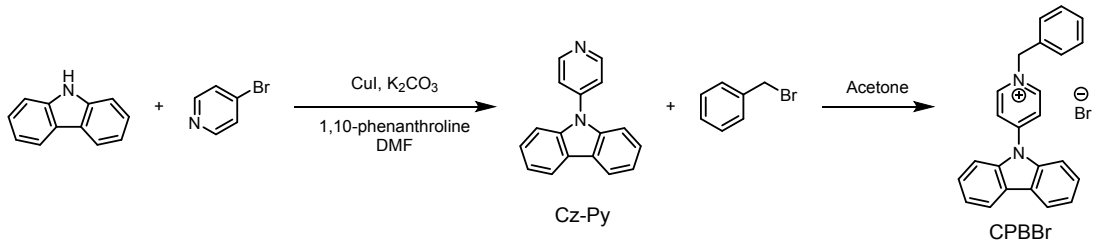

Scheme S1 The synthetic route of CPBBr.

9-(Pyridin-4-yl)-9H-carbazole (Cz-Py): Carbazole (1.672 g, 10 mmol), 4-bromopyridine hydrochloride (2.54 g, 13 mmol), cuprous iodide (0.3 g, 1.6 mmol), 1, 10-phenanthroline (0.6 g, 3.2 mmol), and potassium carbonate (5 g, 40 mmol) were dissolved in the dry DMF (60 ml). The mixed solution was heated to reflux under nitrogen atmosphere for 48 hours. After the reaction, the mixture was cooled to room temperature and ethyl acetate (50 mL) was added, the resultant solution was washed by deionized water for three times (3×100ml), the organic layer was concentrated after dried with anhydrous magnesium sulfate. The crude product was purified by silica gel column chromatography with eluent of hexane/ethyl acetate (20/3, hexane/ethyl acetate) to give Cz-py (1.91 g, 7.80 mmol) as white powder with the yield of 78%. ^{1}H NMR (400 MHz, Chloroform-d) δ (TMS, ppm): 8.88 – 8.81 (m, 2H), 8.17 – 8.10 (m, 2H), 7.62 – 7.56 (m, 2H), 7.55 (t, J = 1.0 Hz, 2H), 7.44 (ddd, J = 8.4, 7.2, 1.4 Hz, 2H), 7.38 – 7.28 (m, 2H)

1-Benzyl-4-(9H-carbazol-9-yl)pyridin-1-ium (CPBBr): Cz-Py (0.488 g, 2 mmol) was dissolved in acetone (8 mL), then the solution of benzyl bromide/acetone (0.708 ml, 6 mmol/5 mL) was added dropwise under magnetic stirring. The resultant mixture was heated to 50 °C and refluxing for 18 h, the product was precipitated. After the precipitate was washed with ether (3×15 ml) for three times, the colorless needle-like solid was obtained (0.751g, 1.81 mmol) with the yield of 90%. ^{1}H NMR (400 MHz, DMSO-d_6) δ (TMS, ppm): 9.29 (d, J = 8 Hz，2H), 8.56 (d, J = 8 Hz, 2H), 8.32 (d, J = 8 Hz, 2H), 7.90 (d, J = 8 Hz, 2H), 7.70 – 7.58 (m, 2H), 7.60 – 7.52 (m, 2H), 7.51 – 7.41 (m, 5H), 5.91 (s, 2H). ^{13}C NMR (101 MHz, DMSO-d_6) δ (ppm): 151.49, 146.84, 138.46, 135.09, 129.86, 129.78, 129.44, 127.81, 125.47, 123.82, 123.10, 121.56, 111.80, 62.58.

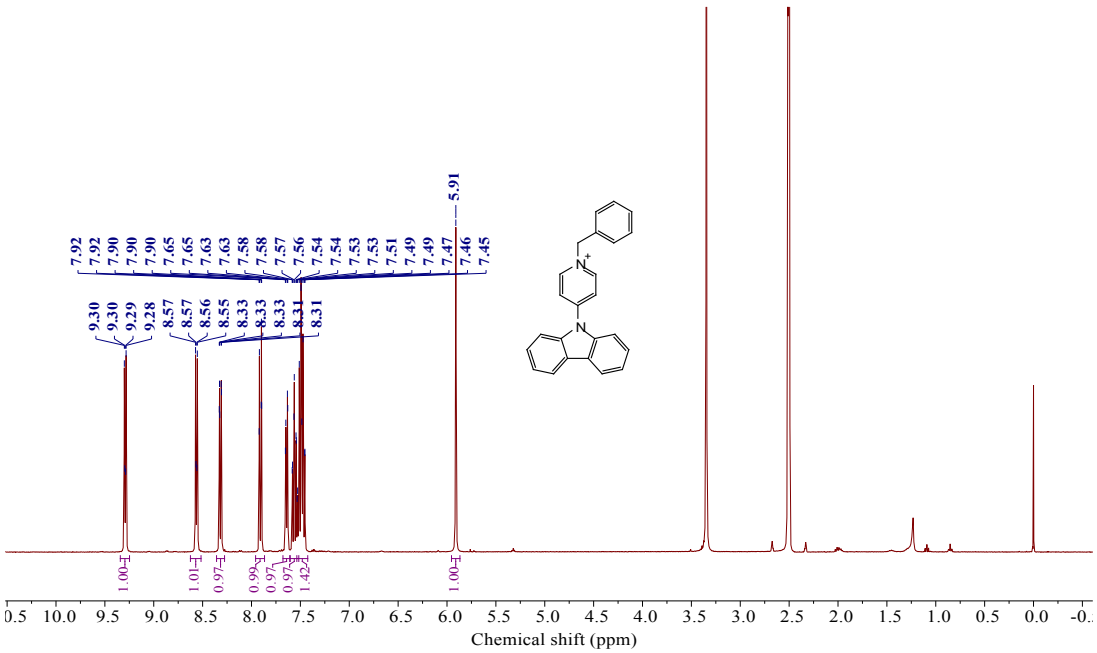

Fig. S1 ^{1}H NMR spectrum of CPBBr in DMSO-d_6 solution

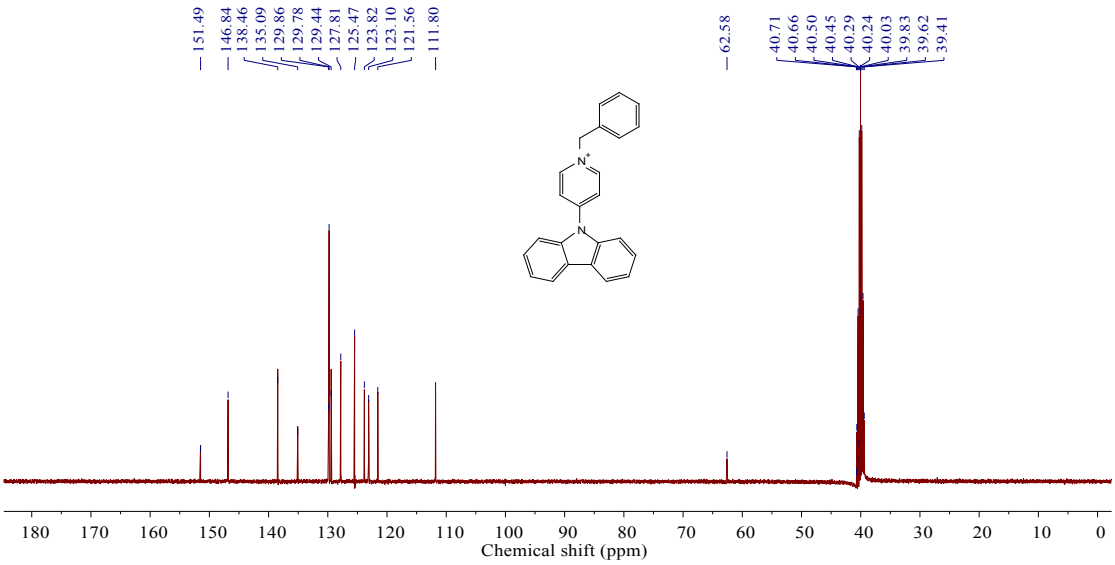

Fig. S2 ^{13}C NMR spectrum of CPBBr in DMSO-d_6 solution

Table S1. The absorption wavelength of CPBBr in various solvents and corresponding E_T^N values.

Solvent	E_T^N	λ_{abs} (nm)
Dichloromethane	0.309	308
N-propanol	0.617	302
Ethanol	0.654	300
Methanol	0.762	297
Water	1.000	291

E_T^N = the normalized Reichardt's parameter

Table S2. PL parameters of CPBBr-W and CPBBr-G in different state.

Compound	λ (nm)	τ (ns)	Φ_{PL} (%)
CPBBr-W	422	1.38	5.8
CPBBr-W-ground	505	1735.29	18.0
CPBBr-G	471	4.14	29.6
CPBBr-G-ground	513	2319.99	25.9
CPBBr-CD	509	6.27	30.6

Φ_{PL}=PL quantum yield, λ_{em}=emission maximum, CD=cyclodextrin. The preparation of CPBBr-CD film: cyclodextrin (CD, 1 mmol) and CPBBr (1 mmol) were dissolved in deionized water (20 mL), the pale-yellow film can be obtained after removing water by rotary evaporation.

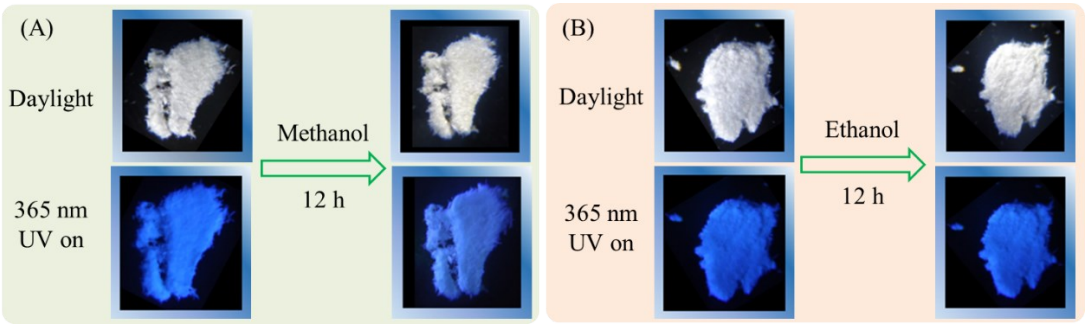

Fig. S3 Daylight and 365 nm UV light photograph of crystallite sample of CPBBr-W under (A) methanol vapor and (B) ethanol vapor at 25 °C in a sealed container.

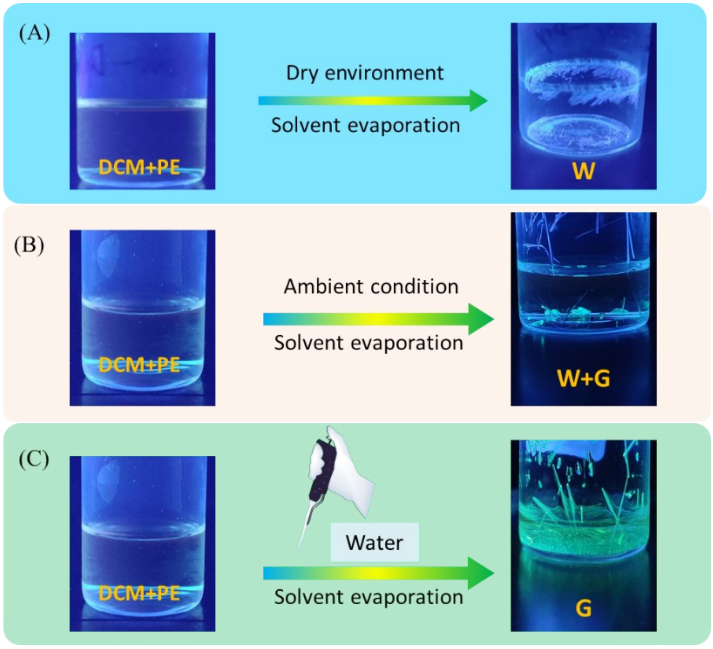

Fig. S4 Single crystal was cultivated by solvent evaporation. (A) In mixture solution of DCM and petroleum ether (PE) (V/V, 1/1) under dry environment, only CPBBr-W crystal was obtained; (B) under ambient condition, both CPBBr-W and CPBBr-G crystals were obtained; (C) when trace amount of water was added in DCM/PE solution, only CPBBr-G crystal obtained.

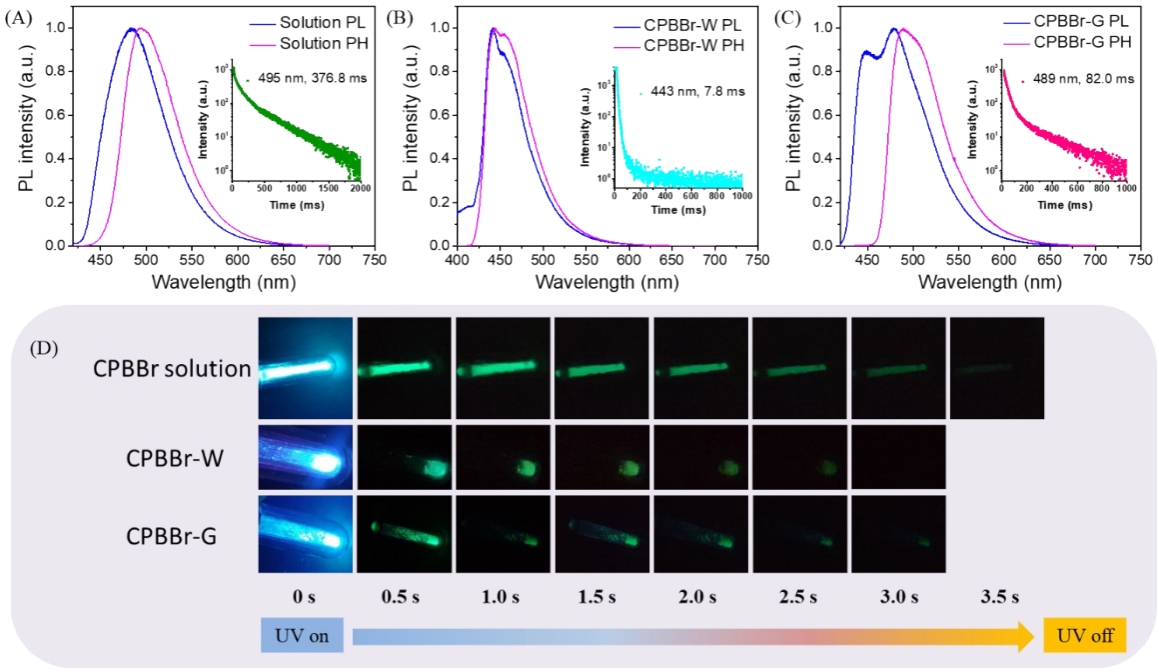

Fig. S5 The PL and phosphorescence (PH) spectra of CPBBr in the DCM solution (3×10^{-5} M) (A), CPBBr-W (B) and CPBBr-G (C) at 77 K, λ_{Ex}=365 nm, inserts show the corresponding time resolved phosphorescence decay curves; (D) Photographs of CPBBr solution, CPBBr-W, and CPBBr-G under 365 nm UV on and UV off at 77 K.

Table S3. The emission maximum of PL, phosphorescence (PH), and phosphorescence lifetime of CPBBr solution (in DCM), CPBBr-W and CPBBr-G at 77 K.

	CPBBr solution	CPBBr-W	CPBBr-G
PL (nm)	484	442	447/479
PH (nm)	495	443	489
τ_{PH} (ms)	376.8	7.8	82.0

Table S4. Unit cell parameters of single crystals of CPBBr-G and CPBBr-W and experimental details

	CPBBr-G	**CPBBr-W**
CCDC number	2068450	2068451
Empirical formula	$C_{24}H_{21}BrN_2O$	$C_{24}H_{19}BrN_2$
Formula weight	433.34	43.72
Temperature (K)	293(2)	293(2)
Crystal system	triclinic	orthorhombic
Space group	P-1	$P2_12_12_1$
a (Å)	7.1414(3)	5.20980(10)
b (Å)	9.7611(4)	13.45740(10)

c (Å)	14.7917(6)	28.7733(3)
α (°)	102.789(4)	90
β (°)	96.075(3)	90
γ (°)	98.261(3)	90
Volume (Å^3)	984.91(7)	2017.31(5)
Z	2	38
ρ_{calc} (g cm^{-3})	1.461	1.367
μ (mm^{-1})	2.969	2.839
F(000)	444.0	848.0
Crystal size (mm^3)	0.4 × 0.3 × 0.2	0.4 × 0.3 × 0.2
Radiation	Cu Kα (λ = 1.54184)	Cu Kα (λ = 1.54184)
2Θ range for data collection (°)	9.432 to 146.18	7.252 to 134.144
Index ranges	-8 ≤ h ≤ 8, -12 ≤ k ≤ 11, -18 ≤ l ≤ 18	-6 ≤ h ≤ 5, -16 ≤ k ≤ 16, -34 ≤ l ≤ 34
Reflections collected	6658	30924
Independent reflections	3819 [R_{int} = 0.0193, R_{sigma} = 0.0262]	3602 [R_{int} = 0.0297, R_{sigma} = 0.0124]
Data/restraints/parameters	3819/0/261	3602/0/244
Goodness-of-fit on F^2	1.070	1.083
Final R indexes [I>=2σ (I)]	R_1 = 0.0312, wR_2 = 0.0827	R_1 = 0.0255, wR_2 = 0.0793
Final R indexes [all data]	R_1 = 0.0335, wR_2 = 0.0848	R_1 = 0.0261, wR_2 = 0.0799

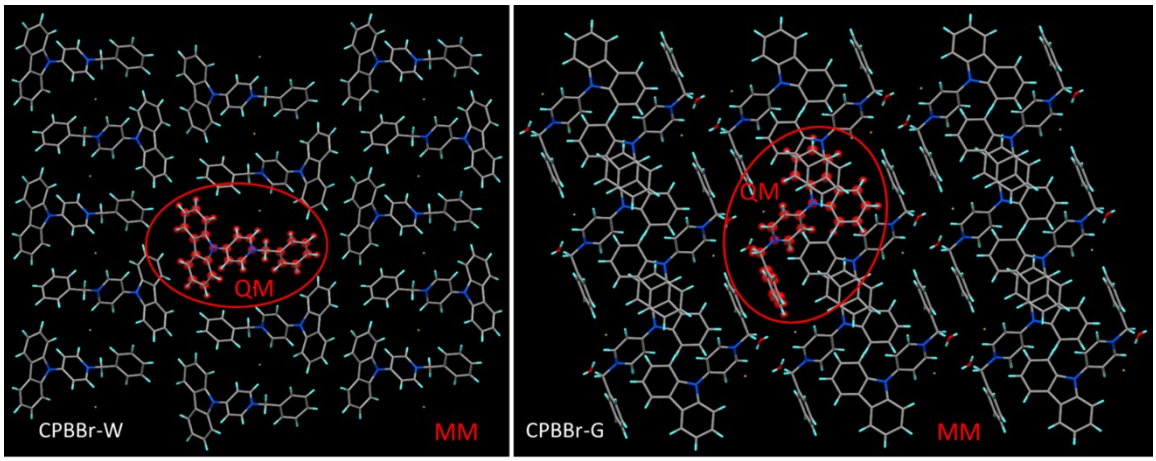

Fig. S6 The ONIOM model of molecular cluster that extracted from single crystal, which compose of 65 molecules for CPBBr-W and 54 molecules for CPBBr-G. The molecule marked in red is divided into high layer and calculated by quantum mechanical (QM) method at DFT/B3LYP/6-31G(d) level, while the rest of molecules are chosen as low layer and simulated via molecular mechanical (MM) method of universal force field (UFF).

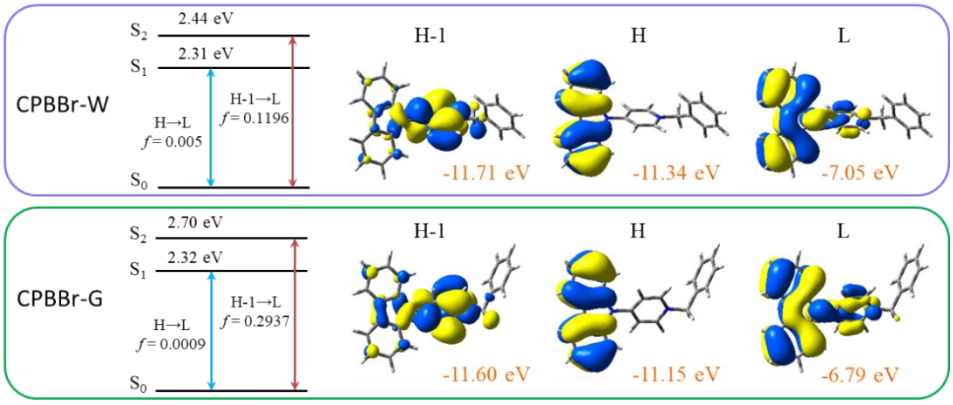

Fig. S7 Molecular energy level of S_0, S_1, and S_2 states, orbital contribution, and oscillator strength (*f*) of CPBBr-W and CPBBr-G, frontier molecular orbitals of HOMO-1 (H-1), HOMO (H), and LUMO (L), the excitation energy is calculated by CAM-B3LYP/6-31G(d) method.

Table S5. The calculated excitation energy of S_1, S_2, and S_3 at optimized S_1 geometry, and the corresponding molecule orbital contribution, oscillator strength (f).

Crystal	n-th transition	Excitation energy (eV)	Molecular orbital contribution	Oscillator strength (*f*)
CPBBr-W	S_1	2.31	H-1→L (0.027), H→L (0.957)	0.005
	S_2	2.44	H-1→L (0.938), H→L (0.028)	0.1196
	S_3	3.76	H-1→L+1 (0.436), H→L+1 (0.545)	0.0008
CPBBr-G	S_1	2.32	H→L (0.984)	0.0009
	S_2	2.70	H-1→L (0.97)	0.2937
	S_3	3.77	H→L+1 (0.989)	0.0003

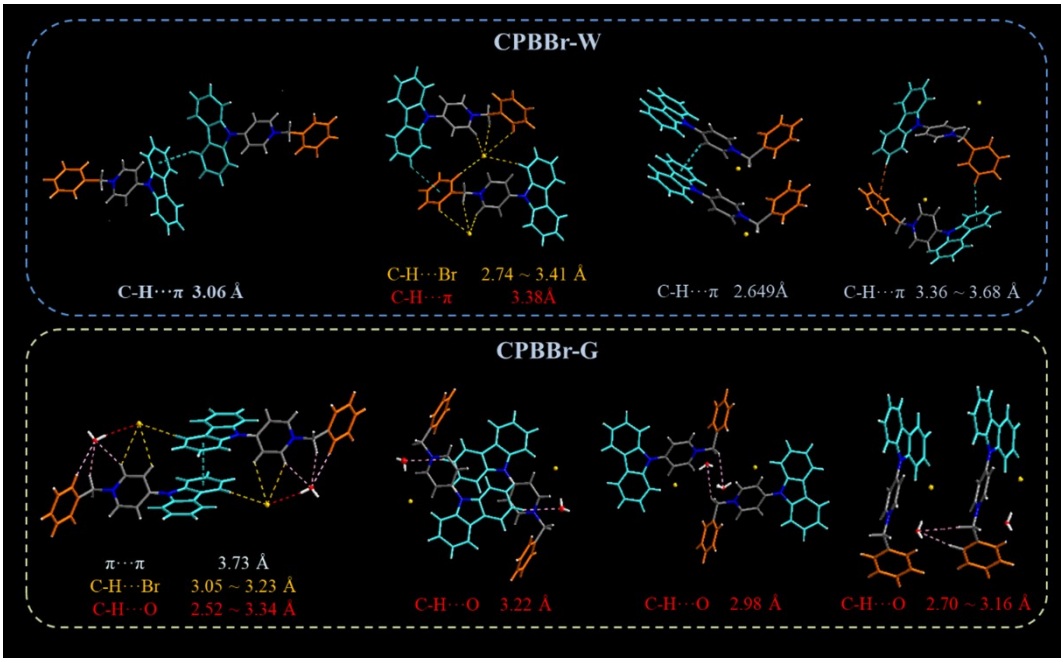

Fig. S8 The intermolecular hydrogen bonding and π···π interaction of dimers that extracted from CPBBr-W and CPBBr-G.

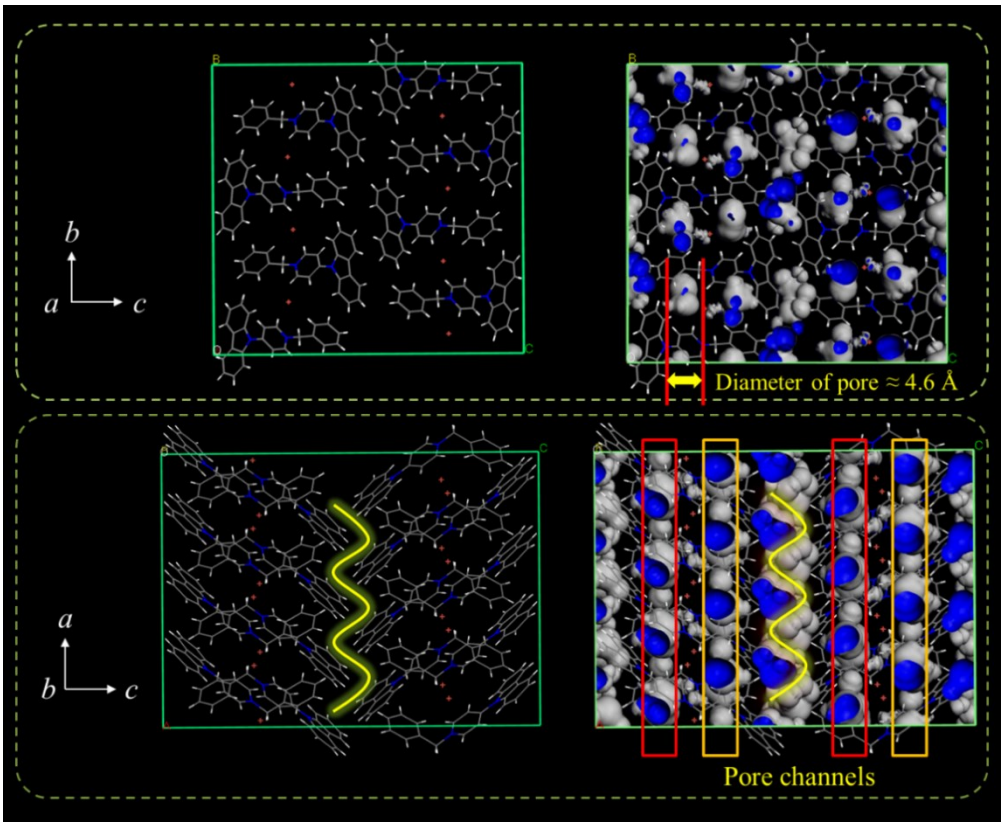

Fig. S9 Schematic presentation of free volume isosurface (0.141) of CPBBr-W from a- and b-axis, lots of pore channels are found along a-axis and near bromide ion, the diameter of pore is about 4.6 Å. The pore channel locates at intersection area of molecular cluster (labelled as yellow line) is crooked and the diameter is less than 3 Å.

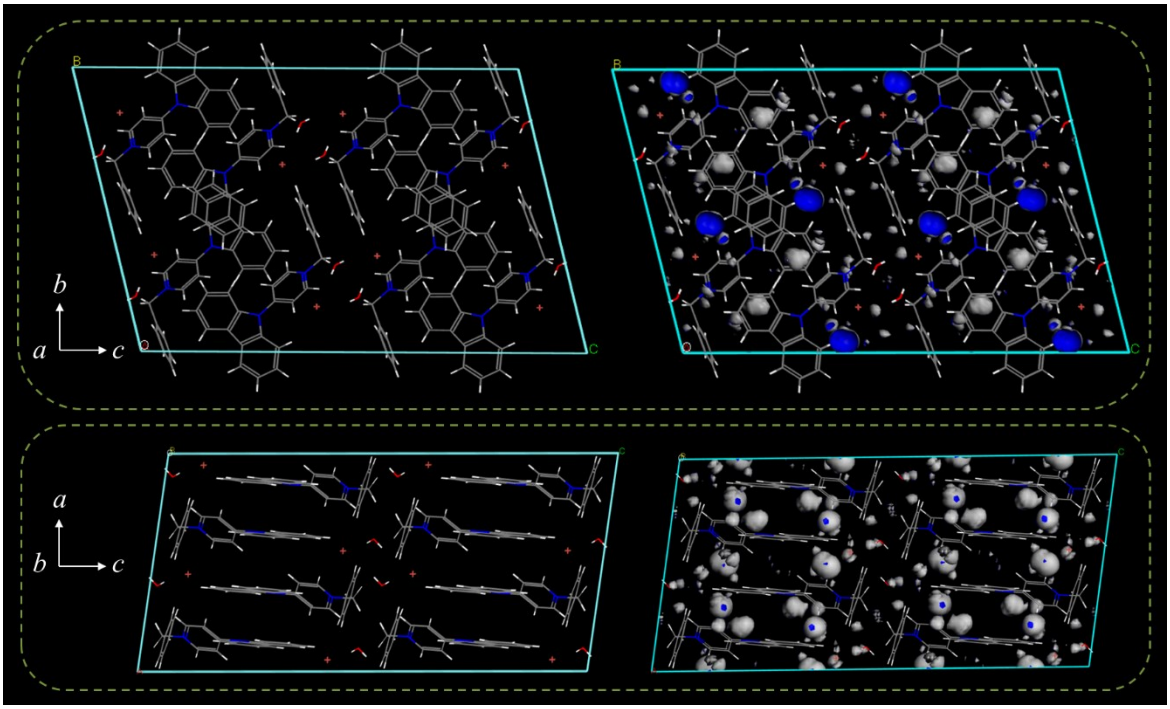

Fig. S10 Schematic presentation of free volume isosurface (0.021) of CPBBr-G from a- and b-axis.

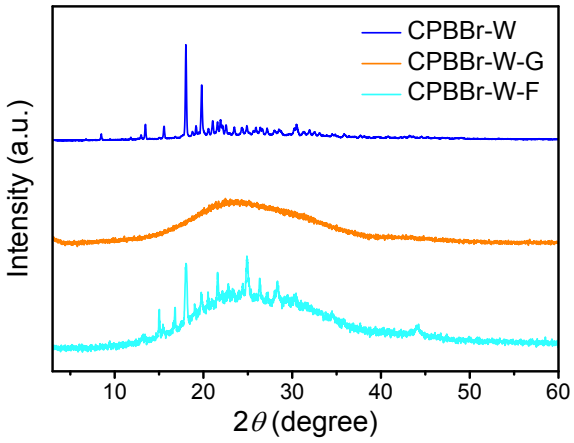

Fig. S11 PXRD patterns of CPBBr-W, ground sample, (CPBBr-W-G), and further fuming by DCM (CPBBr-W-F).

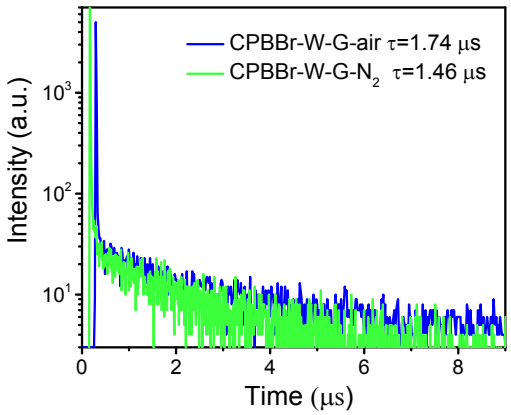

Fig. S12 Fluorescence lifetime of CPBBr-W-G in air and nitrogen (N_2) atmosphere (λ_{Ex}=365 nm).

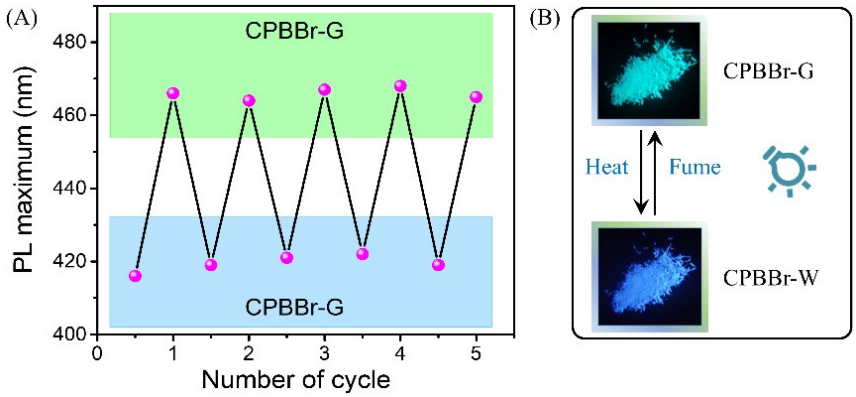

Fig. S13 (A) The PL variation between CPBBr-G and CPBBr-W under cyclic water fuming and heating at 100 °C in a vacuum; (B) photographs of CPBBr-G and CPBBr-W under 365 nm UV light.

Table S6. CIE chromaticity coordinates of CPBBr-W and CPBBr-G under different states.

Compound states	CIE (x, y)	Compound states	CIE (x, y)
CPBBr-W	(0.159, 0.057)	CPBBr-G	(0.170, 0.294)
CPBBr-W-G	(0.248, 0.454)	CPBBr-G-G	(0.277, 0.51)
CPBBr-W-F	(0.164, 0.119)	CPBBr-G-F	(0.170, 0.294)

Reference

1. M. J. Frisch, G. W. Trucks, H. B. Schlegel, G. E. Scuseria, M. A. Robb, J. R. Cheeseman, G. Scalmani, V. Barone, B. Mennucci, G. A. Petersson, H. Nakatsuji, M. Caricato, X. Li, H. P. Hratchian, A. F. Izmaylov, J. Bloino, G. Zheng, J. L. Sonnenberg, M. Hada, M. Ehara, K. Toyota, R. Fukuda, J. Hasegawa, M. Ishida, T. Nakajima, Y. Honda, O. Kitao, H. Nakai, T. Vreven, J. A. Montgomery, Jr., J. E. Peralta, F. Ogliaro, M. Bearpark, J. J. Heyd, E. Brothers, K. N. Kudin, V. N. Staroverov, T. Keith, R. Kobayashi, J. Normand, K. Raghavachari, A. Rendell, J. C. Burant, S. S. Iyengar, J. Tomasi, M. Cossi, N. Rega, J. M. Millam, M. Klene, J. E. Knox, J. B. Cross, V. Bakken, C. Adamo, J. Jaramillo, R. Gomperts, R. E. Stratmann, O. Yazyev, A. J. Austin, R. Cammi, C. Pomelli, J. W. Ochterski, R. L. Martin, K. Morokuma, V. G. Zakrzewski, G. A. Voth, P. Salvador, J. J. Dannenberg, S. Dapprich, A. D. Daniels, O. Farkas, J. B. Foresman, J. V. Ortiz, J. Cioslowski, and D. J. Fox, Gaussian, Inc., Wallingford CT, 2013.